Supplementary Information

A lineage-specific *STAT5B*^{N642H} mouse model to study NK-cell leukemia

This file includes the Supplementary Methods, Supplementary Figures S1-S7, Supplementary Figure Legends, the Supplementary References and an Annex Part I (uncropped western blot membranes).

Supplementary Materials and Methods

Mouse crossing

Homozygous R26-LSL STAT5B^{N642H} knock-in mice (B6-*Gt(ROSA)26Sor*$^{tm1(STAT5B-N642H)}$) were crossed to *Vav*-Cre mice[1]. Their offspring carrying a heterozygous transgene integration at the R26 locus were used for the experiments.

All three homozygous R26-LSL knock-in lines (B6-*Gt(ROSA)26Sor*$^{tm1(STAT5B-N642H)}$, B6-*Gt(ROSA)26Sor*$^{tm2(STAT5B)}$ and B6-*Gt(ROSA)26Sor*$^{tm3(EGFP)}$) were crossed to *Ncr1*-iCreTg mice[2]. Mice carrying a homozygous integration of the transgenes have been used for all experiments with the R26-LSL lines crossed to *Ncr1*-iCreTg mice. Due to heterozygosity of *Ncr1*-iCre expression, the three mouse lines each contained Cre positive littermates (denoted as GFP$^{NK/NK}$ mice for the empty vector control line, STAT5B$^{NK/NK}$ mice for the line with the STAT5B transgene and as N642H$^{NK/NK}$ mice for the line with the STAT5B^{N642H} transgene) and Cre negative littermates lacking transgene expression (denoted as "Cre neg", which represents either a pool of the Cre-negative littermates from all the three different lines (GFP$^{NK/NK}$, STAT5B$^{NK/NK}$ and N642H$^{NK/NK}$ mice) or only N642H$^{NK/NK}$ mice).

Mice were maintained at the rodent facility of the University of Veterinary Medicine Vienna and the specific pathogen-free (SPF) quality of the animals was frequently confirmed according to FELASA recommendations for health monitoring[3]. Animal experiments were discussed and approved by the Ethics and Animal Welfare Committee of the University of Veterinary Medicine Vienna and the national authority (Austrian Federal Ministry of Education, Science and Research) in accordance with good scientific practice guidelines and national legislation, under licenses BMBWF-68.205/0103-WF/V/3b/2015, BMBWF-68.205/0010-V/3b/2019, BMBWF-68.205/0174-V/3b/20182022-0.762.012, 2023-0.108.862, 2022-0.404.452.

Aged mice as well as transplanted recipient mice were monitored daily for the onset of disease signs and sacrificed whenever reaching the pre-defined humane endpoints.

Genotyping PCR

PCR reactions were prepared on ice as follows: 1x Buffer II (Roche), 1 µM primer mix (R26_wt_rev, R26_wt_fw, R26_EGFP_fw), 2 mM dNTPs (Fermentas), 0.1 µl AmpliTaq DNA Polymerase (5U/µl), ddH2O per sample were added to a final of 20 µl reaction. The reaction was run at 95 °C (30 sec), 65 °C (30 sec) and 72 °C (40 sec) for 35 cycles on an Eppendorf Mastercycler. Each PCR product was mixed with 5 µl 6x DNA loading dye. 25 µl were loaded on a 1.5% (w/v) agarose gel immersed in 50x Tris Acetate (TAE) buffer until appropriate separation occurred. DNA was visualized with ethidium bromide in TAE Gel (1:20,000)

exposed to ultraviolet (UV) light in a Gel Doc™ XR Imager (Biorad). As reference marker the Gene RulerTM 1000 bp DNA ladder (Thermo Scientific) was used.

Cell lines

LentiX293T cells (Addgene) were cultured with DMEM (Sigma) complete medium, containing 10% FCS (Bio&Sell), 100 U/mL penicillin, 100 µg/mL streptomycin (Sigma), and 50 µM β -mercaptoethanol (Sigma).

Parental and transduced KHYG-1[4] (purchased from DSMZ) and IMC-1[5] (kindly provided by Prof. Chen, University of New Mexico Comprehensive Cancer Center) human NK-cell lines were cultured with RPMI complete with 100 U/ml, 25 U/ml or without human IL-2 (Proleukin, SteriMax).

Lentiviral transduction of human NK-cell lines

Human non-mutant (WT) *STAT5B* or *STAT5B*^{N642H} transgenes were cloned into a pWPI lentiviral expression vector (Addgene plasmid # 12254; kindly provided by the lab of Prof. Hoermann, previously at the Department of Laboratory Medicine, Medical University of Vienna), allowing for transgene expression coupled to IRES-controlled GFP expression. An empty vector control for expression of IRES-controlled GFP alone was included. Lentiviruses were generated by transfection of 4 µg of pWPI vectors (carrying the transgenes or the empty vector as a control) together with 3 µg of packaging vectors (2 µg of psPAX2 (Addgene plasmid # 12260) and 1 µg of pMD2.G (Addgene plasmid # 12259); kindly provided by Prof. Grebien, University of Veterinary Medicine Vienna) using Turbofect (Thermo Fisher Scientific) into around 80% confluent LentiX cells. 24h after the transfection, the medium was exchanged to RPMI complete medium containing 30 % FCS. After another 24h, supernatants were filtered through a 0.45-µm filter and used for the first round of lentiviral transduction. 3*10^5 KHYG-1 or IMC-1 cells were resuspended in 1.5 ml of each of the lentiviral supernatants, supplemented with 100 U/ml IL-2 and 4 µg/ml Polybrene (Sigma), and seeded into 12-well plates. Spinoculation was performed for 90 minutes at 1000g. After centrifugation, cells were incubated at 37°C and 5% CO2. On the next day, the transduced KHYG-1 and IMC-1 cells were washed and a second round of lentiviral transduction was performed with the lentiviral supernatants collected from the same LentiX cells (around 65-70h after transfection). After an overnight incubation at 37 °C, the remaining virus supernatant was washed away, and transduced KHYG-1 and IMC-1 cells were continued to be cultured in RPMI complete supplemented with 100 U/ml IL-2. To test how overexpression of WT STAT5B and the STAT5B^{N642H} mutant impact on the growth of the transduced human NK-cell lines at a reduced IL-2 concentration, the transduced cell lines were cultured in parallel with 25 U/ml or 100U/ml

IL-2, starting from four days after the second lentiviral infection (4 days post infection (*p.i.*)). At 19 days *p.i.*, transduced cell lines that were cultured at 25 U/ml IL-2 were completely deprived of IL-2. The viability of the transduced human NK-cell lines was analyzed at multiple timepoints after IL-2 withdrawal by flow cytometry, using SYTOX™ Blue Dead Cell stain (Thermo Fisher Scientific) as a viability dye. Additionally, their percentages of GFP positivity were determined as a surrogate for transgene expression.

Transplantation experiments

For transplantation experiments from diseased N642H$^{vav/+}$ and N642H$^{NK/NK}$ mice, 2.5×10^5-5×10^6 splenocytes from diseased mice or control mice were injected intravenously (*i.v.*) into NSG (NOD.Cg-Prkdc^{scid} Il2rg^{tm1}Wjl/SzJ) or Ly5.1 recipient mice.

Four transduced human NK-cell lines were selected in addition to the parental cell lines for transplantation into NSG mice. KHYG-1 +STAT5B^{N642H} and IMC-1 +STAT5B^{N642H} represent cells overexpressing the STAT5B^{N642H} mutant that were obtained upon culture without IL-2, showing > 94 % transgene expression (evaluated by GFP positivity). The control cells overexpressing non-mutant STAT5B (KHYG-1 +STAT5B and IMC-1 +STAT5B) were sorted to achieve a > 98% transgene expression (evaluated by GFP positivity). The sorted KHYG1 +STAT5B cells were cultured at 100 U/ml IL-2, while IMC-1 +STAT5B cells could be maintained at 25 U/ml IL-2. 1-3×10^6 of these transduced human NK cell lines were injected *i.v.* into NSG recipient mice.

All transplanted mice were monitored daily for onset of disease symptoms and sacrificed once they reached the humane endpoints.

Hematocytometry and Flow Cytometry

Blood was collected into EDTA tubes (Greiner Bio-One Mini-Collect K3EDTA Tubes (Thermo Fisher Scientific)) from the V. *facialis* or via cardiac puncture under terminal anesthesia. White blood cell (WBC), lymphocyte (LYM), platelet (PLT) counts and haematocrit (HCT) were measured using an animal blood counter (scil Vet ABC).

For flow cytometric analysis, single cell suspensions were prepared from spleens, livers (LIV), bone marrow (BM), lymph nodes (LN) and lungs. Isolation of hepatic leucocytes was performed by separation with 37.5% percoll (GE Healthcare, Chicago, Illinois, USA). Lysis of erythrocytes from single cell suspension of BM, spleen and liver was performed with Red blood cell Lysis Buffer (150 mM NH4Cl, 10 mM KHCO3, 0.1 mM Na2EDTA, pH 7.2-7.4) prior to incubation with fluorescently labelled antibodies. For blood analysis, erythrocyte lysis was performed after the antibody staining.

Purified anti-CD16/CD32 antibodies (clone 93; Thermo Fisher Scientific (eBioscience™)) were used for blocking of Fc receptors.

Fluorochrome-conjugated antibodies (clones) directed against following proteins were purchased from ThermoFisher Scientific (eBioscience™): CD4 (GK1.5), CD8a (53-6.7), CD11b (M1/70), CD19 (eBio1D3), CD34 (RAM34), CD45.2 (104), CD122 (5H4), CD135 (A2F10), c-kit (2B8), Gr-1 (RB6-8C5), NKp46 (29A1.4), Sac-1 (D7), Ter119 (TER-119); from Biolegend/Biozym: CD3 (17A2), CD3e (145-2C11), CD25 (PC61), CD44 (IM7), CD48 (HM48-1), CD90.2 (53-2.1), CD150 (TC15-12F12.2), NK1.1 (PK136), TCRβ (H57-597), TCRγδ (GL3); or from Miltenyi Biotec: CD27 (REA499), KLRG1 (REA1016), KLRG1 (2F1/KLRG1), CD49a (Ha31/8), CD49b (DX5), CD27 (LG.7F9), NKG2D (CX5).

Analysis of apoptosis of splenic NK cells was performed *ex vivo* by staining with AnnexinV and 7-AAD using Annexin V Apoptosis Detection Kits (Thermo Fisher Scientific) according to the manufacturer's protocol.

For intracellular staining of perforin (clone S1600A, Biolegend) and pYSTAT5 (clone 47, BD), splenocytes were fixed with 2% paraformaldehyde (Sigma) after staining for surface markers and permeabilized with ice-cold 90% methanol before intracellular stainings. For detection of intracellular granzyme B (clone NGZB, Thermo Fisher Scientifc (eBioscience^{TM})), BD Cytofix/Cytoperm^{TM} Fixation/Permeabilization Solution Kit (BD Bioscience) was used according to manufacturer's instructions.

Total cell numbers were assessed by flow cytometry using Count Bright Beads (Invitrogen).

Flow cytometry samples were acquired using a Cytoflex (Beckman Coulter) or Cytoflex S (Beckman Coulter) flow cytometer. Data were analyzed using CytExpert (Beckman Coulter) or FlowJo software.

Histology

Organs were fixed overnight in 4% phosphate buffered formaldehyde solution (Roti®Histofix, Carl Roth, Karlsruhe, Germany), dehydrated, embedded and cut (4 µm). Paraffin-embedded sections were stained with hematoxylin and eosin (H&E) according to standard histological procedures. Blood smears were stained using a Hemacolor® Rapid staining of blood smears kit (Sigma, St. Louis, Missouri, USA). Images were taken using an Olympus IX71 or an Olympus BX51 microscope (Olympus, Tokyo, Japan) equipped with a Olympus UC90 camera and CellSens Entry Software 2.3. Adobe Photoshop was used for optimization of color contrast.

Establishment of N642H$^{NK/NK}$ leukemia cell lines and assessment of cytokine-dependent growth

To establish cell lines from the diseased N642H$^{NK/NK}$ NK cells before and after transplantation, cell suspensions of liver, spleen or BM were cultured at a cell concentration of around 1*10^6/ml in RPMI complete medium supplemented with 1500U/ml recombinant human IL-2 (Proleukin, Novartis). Outgrowth of cell lines, with a high purity of GFP+ cells (>95%), was detected after around 3-6 weeks of culture. Cell lines could successfully be resuscitated after freezing and thawing. To test IL-2 dependency, the cell lines were washed and cultured with different IL-2 concentration or without IL-2 as indicated in **Figure S6O**. Cell numbers and viability were monitored every 2-3 days for a period of 9-11 days by flow cytometry. Cell counts as depicted in the growth curves (**Figure S6O**) represent the absolute numbers of viable cells.

NK-cell culture

Splenic NK cells were isolated using DX5-labeled MACS beads according to the manufacturer's instructions (Miltenyi Biotec). NK cells were cultured for up to 7 days in RPMI complete medium (10% FCS (Bio & Sell), 100 U/mL penicillin (Sigma), 100 µg/mL streptomycin (Sigma), 50 µM β -mercaptoethanol (Sigma)) supplemented with 400ng/ml murine (m)IL-2 (kindly provided by Peter Steinlein, Research Institute of Molecular Pathology (IMP)).

Cytokine stimulation of splenocytes or cultured NK cells

For *ex vivo* analysis of pYSTAT5 dephosphorylation by intracellular flow cytometry, splenocytes were stimulated with 20 ng/ml mIL-15 (PeproTech) for 20 min. Cells were washed twice with PBS and then cultured in RPMI complete medium (without cytokines) for 0, 30, 60, 90, 120 and 240 mins. Upon starvation, cells were harvested and processed for intracellular flow cytometry.

For analysis of pYSTAT5 levels by immunoblotting, NK cells were cultured with IL-2 for 7 days and either directly lysed or lysed after 3h of IL-2 withdrawal with or without restimulation with 400 ng/ml mIL-2 and 50 ng/ml mIL-15 (PeproTech) for 20min.

Immunoblotting

Protein lysates from BM cells or IL-2 cultured NK cells were prepared in 1x Laemmli buffer, heated at 95°C for 5 min and sonicated at room temperature for 15 min. Protein concentrations were assessed using the Pierce™ BCA Protein Assay Kit (Thermo Fisher Scientific). Proteins were separated on 8-10% SDS polyacrylamide gels and transferred onto nitrocellulose membranes (Whatman®Protran®), which were blocked in 5% milk in pY-TBST buffer (10 mM Tris/HCl pH 7.4, 75 mM NaCl, 1 mM EDTA, 0.1% Tween-20). Membranes were incubated with antibodies against tyrosine-phosphorylated (pY-)STAT5 (Y694/699) (clone 47,

BD Biosciences), total (t-)STAT5 (clone C-17, Santa Cruz or polyclonal IgG, R&D (cat. no. AF2168)), V5 (clone V5-10, Sigma Aldrich) overnight. β-Actin (clone AC-15, Santa Cruz) or α -Tubulin (clone 11H10, Cell Signaling Technology (CST)) served as loading controls. For detection of bound primary antibodies, membranes were incubated with horseradish peroxidase-conjugated anti-rabbit or anti-mouse antibodies (CST) followed by chemiluminescent imaging using Clarity Western ECL substrate (BioRad) and the ChemiDoc™ Touch Imaging System (BioRad). Image Lab software (BioRad) was used to process images and band intensity was quantified using the ImageJ Software.

RNA-Seq analysis of aged mouse NK cells

Trimmomatic (version 0.39)[6] was used for read filtering and umi-tools (version 1.1.4)[7] was used to remove unique molecular identifier sequences. The quality-controlled and filtered reads were then aligned against the mouse reference genome sequence (GRCm38, primary assembly) using STAR version 2.7.6a[8]. The gene model used was the Gencode-M25 primary assembly annotation[9]. Reads were counted using the featureCounts function from the Subread 2.0.1 package[10]. Differential gene expression analysis was performed in R (Version 4.3.1)[11]. R Foundation for Statistical Computing, Vienna, Austria) with the DESeq2 package[12]. Normalized fragment counts were calculated by multiplying raw fragment counts with size factors, as implemented in DESeq2.

Gene Set Enrichment Analysis (GSEA)

For GSEA, ranked gene lists were prepared from the results of the differential gene expression analysis. We used sign(log2FoldChange) *(-1) *log10(p-value) as the rank metric for each gene ("log2FoldChange" and "p-value" were taken from the DESeq2 results object). GSEA was then performed using the GSEA software (version 4.3.2)[13,14]. Enrichment of gene set collections from HALLMARK MSigDB (version 7.2) was tested[15,16]. The analysis was performed using the command-line script and the "GSEAPreranked" analysis mode. To map mouse ensembl gene IDs to human gene symbols we used the gene annotation chip-file provided with MSigDB after removal of duplicate mappings. The "collapse" parameter was set to "Remap_Only" and the "scoring_scheme" parameter to "classic". For GSEA analysis of the human dataset the "collapse" parameter was set to "No_Collapse".

Supplementary Figures

Figure S1: N642H$^{vav/+}$ mice develop a hematopoietic malignancy

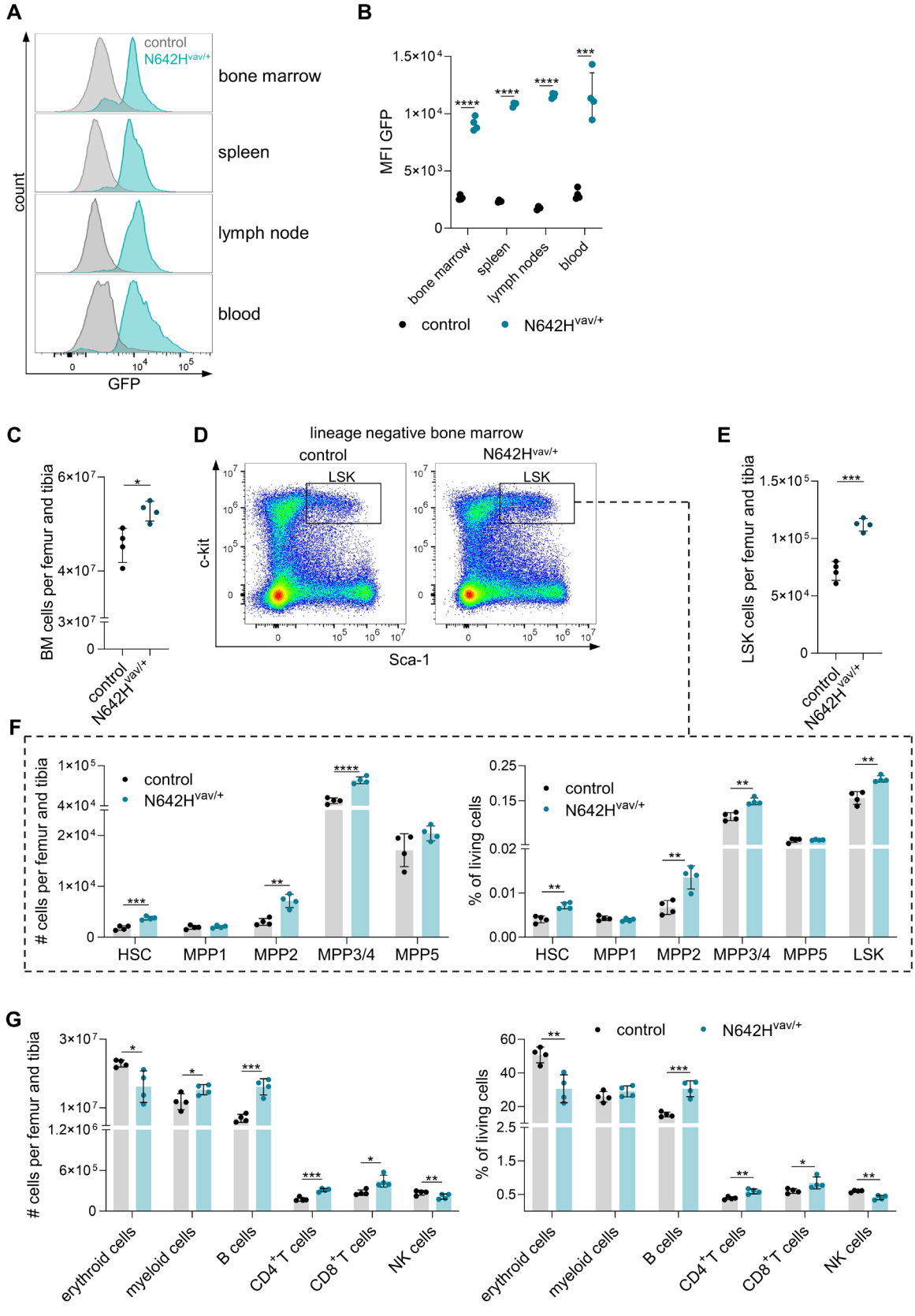

Figure S1: N642H$^{vav/+}$ mice develop a hematopoietic malignancy

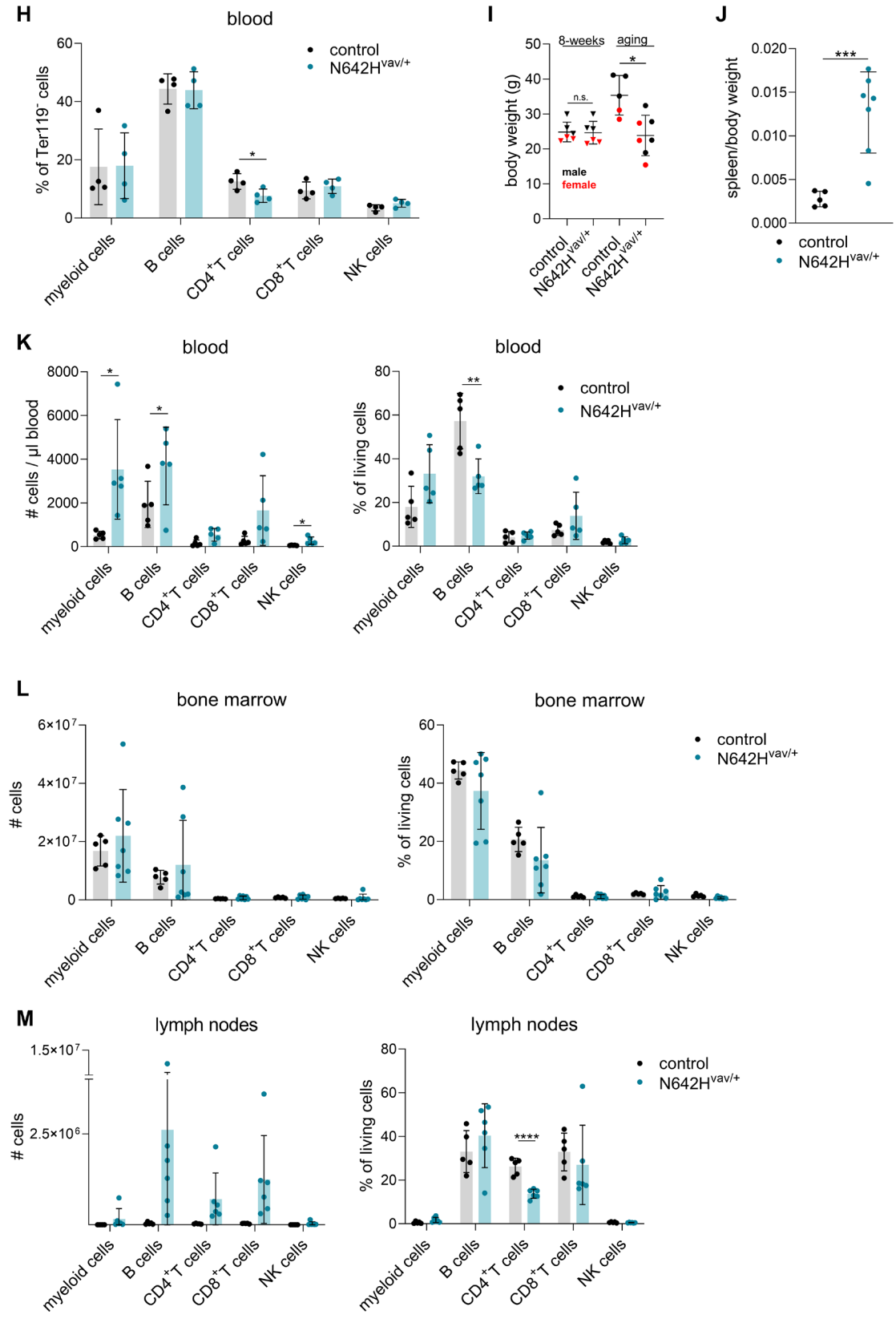

Figure S1. N642H$^{vav/+}$ mice develop a hematopoietic malignancy

(A)-(B) Flow cytometric analysis of GFP levels in different tissues of 8-week-old control and N642H$^{vav/+}$ mice. (A) Representative histograms and (B) quantification of GFP signals in bone marrow (BM), spleen, lymph nodes (LN) or blood from 8-week-old control and N642H$^{vav/+}$ mice (n=4/genotype, mean±SD). (C)-(G) Flow cytometry analyses of BM from 8-week-old control and N642H$^{vav/+}$ mice (n=4/genotype, mean±SD). Quantification of (C) total BM cell numbers, (D) representative gating of LSK population on lineage negative BM cells and (E) total LSK cell numbers. (F) (*Left*) Total cell numbers and (*Right*) relative quantification (percentages out of living cells) of HSC and MPP1-5 cells. HSC subpopulations: HSC (LSK, CD34$^-$CD48$^-$CD150$^+$CD135$^-$), multipotent progenitor (MPP)1 (LSK, CD34$^+$CD48$^-$CD150$^+$CD135$^-$), MPP2 (LSK, CD34$^+$CD48$^+$CD150$^+$CD135$^-$), MPP3/4 (LSK, CD34$^+$CD48$^+$CD150$^-$). (G) (*Left*) Total cell numbers and (*Right*) relative quantification of erythroid cells (Ter119$^+$), myeloid cells (CD11b$^+$Gr1$^+$), B cells (CD19$^+$), CD4$^+$ T cells (CD3$^+$CD4$^+$), CD8$^+$ T cells (CD3$^+$CD8$^+$) and NK cells (CD3$^-$NK1.1$^+$). (H) Relative quantification (percentages out of Ter119 negative cells) of myeloid cells (CD11b$^+$Gr1$^+$), B cells (CD19$^+$), CD4$^+$ T cells (CD3$^+$CD4$^+$), CD8$^+$ T cells (CD3$^+$CD8$^+$) and NK cells (CD3$^-$NK1.1$^+$) in the blood of 8-week-old control and N642H$^{vav/+}$ mice (n=4/genotype, mean±SD). (I) Body weight quantification of 8-week-old control and N642H$^{vav/+}$ mice and aged control (~360 days old) and diseased N642H$^{vav/+}$ mice (142-363 days old, endpoint analysis) (n≥5/genotype, mean±SD). (J) Relative quantification of spleen weights of aged control and diseased N642H$^{vav/+}$ mice (n≥5/genotype, mean±SD). (K) (*Left*) Total cell numbers and (*Right*) relative quantification (percentages out of living cells) of myeloid cells (CD11b$^+$Gr1$^+$), B cells (CD19$^+$), CD4$^+$ T cells (CD3$^+$CD4$^+$), CD8$^+$ T cells (CD3$^+$CD8$^+$) and NK cells (CD3$^-$NK1.1$^+$). in the blood of aged control and diseased N642H$^{vav/+}$ mice (n≥5/genotype, mean±SD). (L) (*Left*) Total cell numbers and (*Right*) relative quantification of myeloid cells (CD11b$^+$Gr1$^+$), B cells (CD19$^+$), CD4$^+$ T cells (CD3$^+$CD4$^+$), CD8$^+$ T cells (CD3$^+$CD8$^+$) and NK cells (CD3$^-$NK1.1$^+$). in the bone marrow of aged control and diseased N642H$^{vav/+}$ mice (n≥5/genotype, mean±SD). (M) (*Left*) Total cell numbers and (*Right*) relative quantification of myeloid cells (CD11b$^+$Gr1$^+$), B cells (CD19$^+$), CD4$^+$ T cells (CD3$^+$CD4$^+$), CD8$^+$ T cells (CD3$^+$CD8$^+$) and NK cells (CD3$^-$NK1.1$^+$) in the lymph nodes of aged control and diseased N642H$^{vav/+}$ mice (n≥5/genotype, mean±SD).

Levels of significance were calculated using unpaired t-test in (B)-(C) and (E)-(M). *$p < 0.05$, **$p < 0.01$, ***$p < 0.001$ and ****$p < 0.0001$.

Figure S2: Leukemic N642H$^{vav/+}$ T-/NKT cells expand upon transplantation

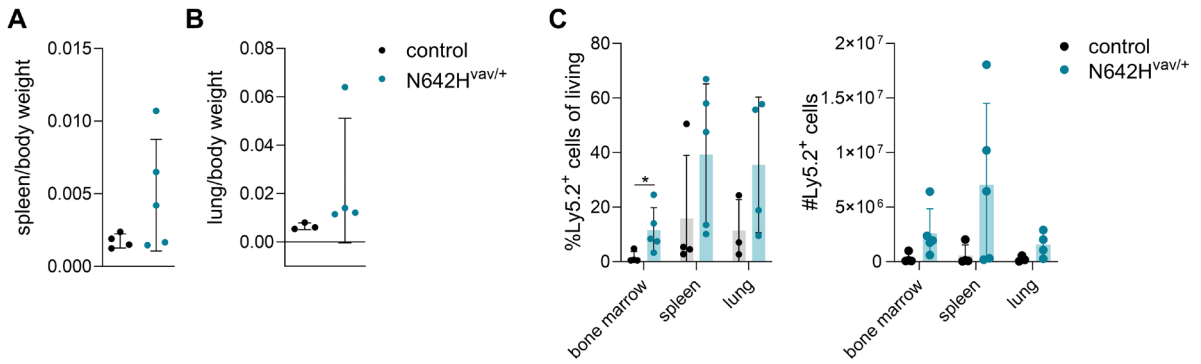

Figure S2: Leukemic N642H$^{vav/+}$ T-/NKT cells expand upon transplantation

Relative quantification of (A) spleen and (B) lung weights of NSG recipient mice injected with control or N642H$^{vav/+}$ cells (n≥3/genotype, mean±SD). (C) (*Left*) Relative quantification (percentages out of living cells) and (*Right*) total numbers of transplanted Ly5.2^{+} cells in BM, spleen and lung of NSG recipient mice (n≥3/genotype, mean±SD).

Levels of significance were calculated using Mann-Whitney test in (C). *p < 0.05.

Figure S3: *STAT5B*^{N642H} promotes cytokine independence of leukemic human NK cells

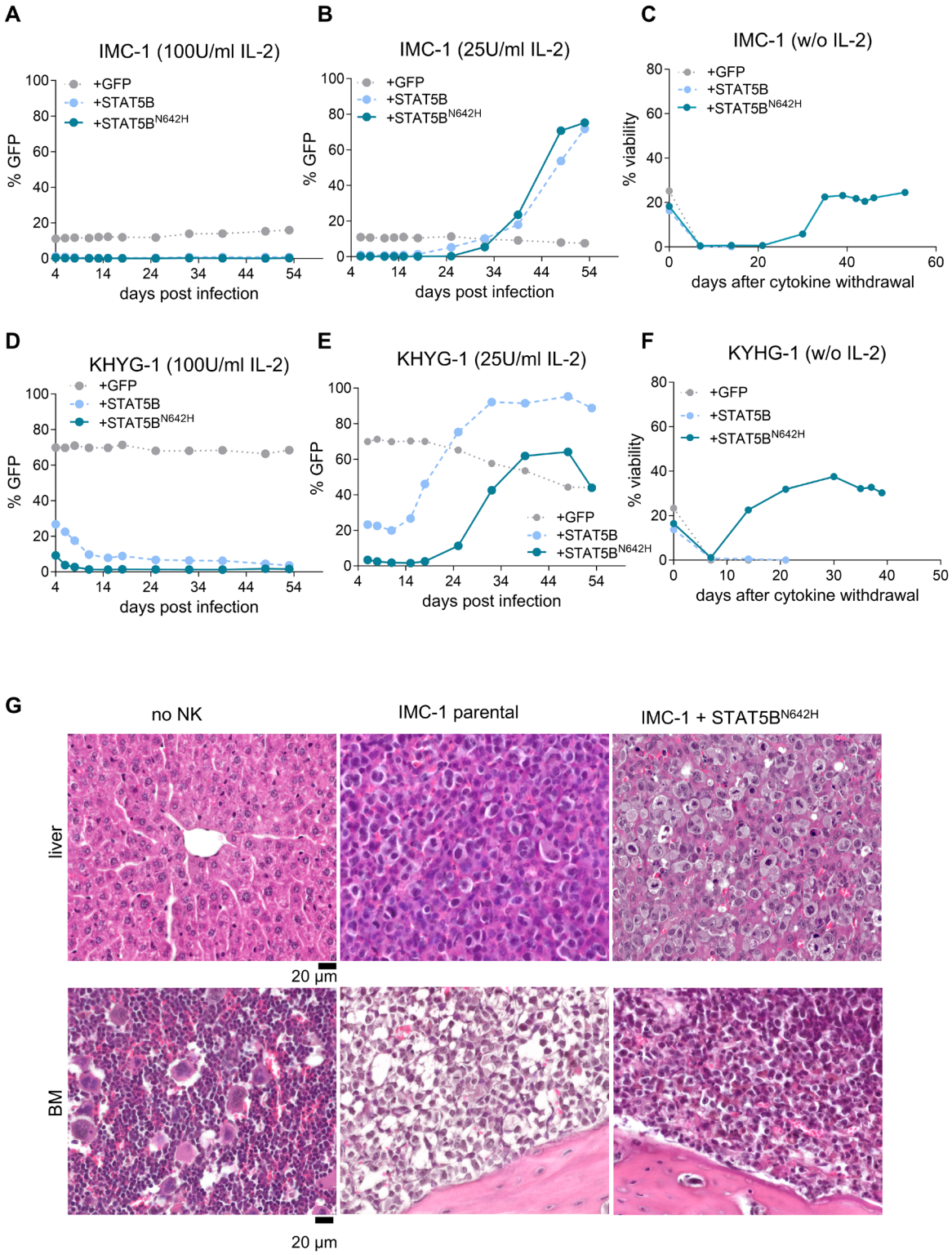

Figure S3. *STAT5B*^{N642H} promotes cytokine independence of leukemic human NK cells

(A-C) IMC-1 and (D-F) KHYG-1 cell lines were transduced with empty vector (+GFP), non-mutant STAT5B (+STAT5B) or STAT5B^{N642H} (+STAT5B^{N642H}). Four days after transduction, cells were either continued to be cultured with (A, D) 100 U/ml IL-2 or at a reduced concentration of concentration of (B, E) 25 U/ml IL-2. (A-B, D-E) Percentage of GFP^{+} cells was monitored over time. After complete IL-2 withdrawal, viability of transduced (C) IMC-1 and (F) KHYG-1 cells was analyzed. (G) Representative images of H&E-stained liver and BM tissue from untransplanted (no NK) NSG mice and NSG mice transplanted with non-transduced (IMC-1 parental) or STAT5B^{N642H} transduced IMC-1 cells (IMC-1 + STAT5B^{N642H}).

Figure S4: An NKp46⁺-cell specific mouse model to study the oncogenic role of *STAT5B*^{N642H} in NK cells

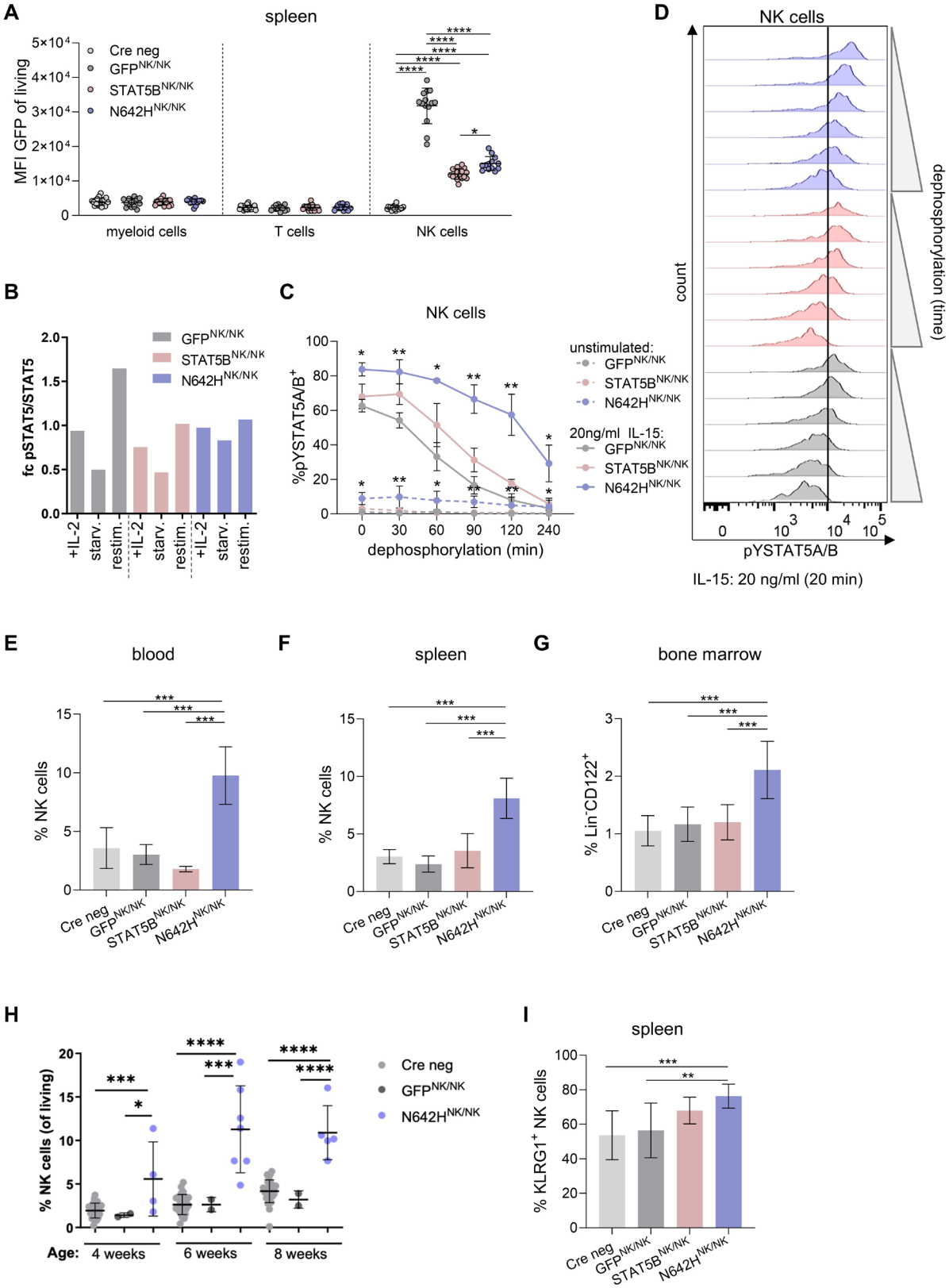

Figure S4: An NKp46^{+}-cell specific mouse model to study the oncogenic role of *STAT5B*^{N642H} in NK cells

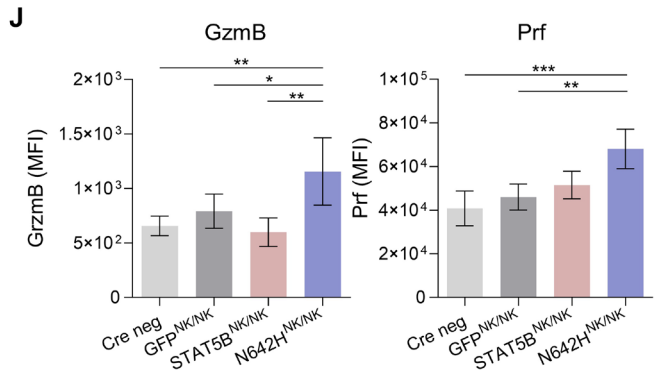

Figure S4. An NKp46^{+}-cell specific mouse model to study the oncogenic role of *STAT5B*^{N642H} in NK cells

(A) Quantification of GFP levels (MFI) in CD3^{-}NK1.1^{-}CD11b^{+} myeloid cells, CD3^{+}NK1.1^{-} T cells and CD3^{-}NK1.1^{+} NK cells in the spleen of GFP$^{NK/NK}$, STAT5B$^{NK/NK}$, N642H$^{NK/NK}$ and Cre neg mice (n≥10/genotype, mean±SD). (B) Quantification of fold change (fc) of pY-STAT5 over total STAT5A/B levels from immunoblot shown in Figure 4B. (C-D) Flow cytometric analysis of *ex vivo* pY-STAT5 levels in unstimulated and IL-15 (20ng/ml) stimulated splenic NK cells from GFP$^{NK/NK}$, STAT5B$^{NK/NK}$ and N642H$^{NK/NK}$ mice over time after washing away cytokine stimulation (0-240min). Dephosphorylation kinetics are depicted as (C) bar graphs (n=3/genotype, mean±SD) and (D) representative histograms. Percentage of NK cells (CD3^{-}NK1.1^{+}NKp46^{+}) in (E) blood and (F) spleen of 8-12-week-old GFP$^{NK/NK}$, STAT5B$^{NK/NK}$, N642H$^{NK/NK}$ and Cre negative (neg) control mice (n≥5/genotype, mean±SD). (G) Percentage of Lin^{-}CD122^{+} cells in BM of GFP$^{NK/NK}$, STAT5B$^{NK/NK}$, N642H$^{NK/NK}$ and Cre neg mice (n≥6/genotype, mean±SD). (H) Quantification of relative abundance (percentage out of living cells) of NK cells (CD3^{-}NK1.1^{+}NKp46^{+}) in the blood of 4-, 6- and 8-week-old Cre neg (n=29), GFP$^{NK/NK}$ (n=2) and N642H$^{NK/NK}$ (n=4-7) mice (mean±SD). (I) Percentages of KLRG1^{+} NK cells in the spleens of GFP$^{NK/NK}$, STAT5B$^{NK/NK}$, N642H$^{NK/NK}$ and Cre neg mice (n≥10/genotype, mean±SD). (J) Steady-state levels of (*Left*) granzyme B (GzmB) and (*Right*) perforin (Prf) in splenic NK cells from GFP$^{NK/NK}$, STAT5B$^{NK/NK}$, N642H$^{NK/NK}$ and Cre neg mice (n≥4/genotype, mean±SD).

Levels of significance were calculated using one-way ANOVA in (A) and (E)-(J) and using Kruskal-Wallis test for each time point in (C). *p < 0.05, **p < 0.01, ***p < 0.001, ****p < 0.0001.

Figure S5: *STAT5B*^{N642H} induces NK-cell leukemia in mice

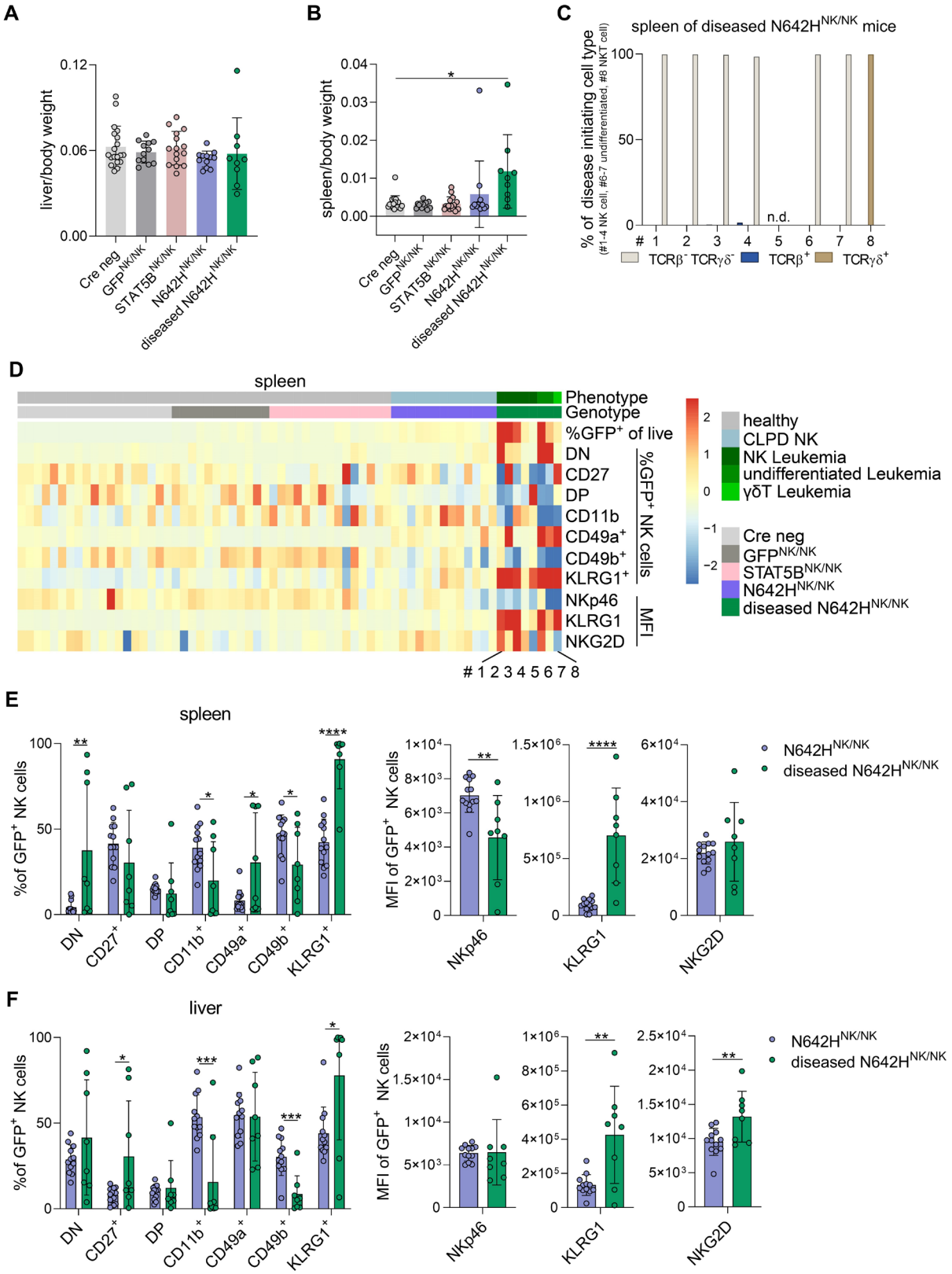

Figure S5. *STAT5B*^{N642H} induces NK-cell leukemia in mice

Quantification of the (A) liver and (B) spleen to body weight ratio of Cre neg, GFP$^{NK/NK}$, STAT5B$^{NK/NK}$, non-diseased N642H$^{NK/NK}$ and diseased N642H$^{NK/NK}$ mice (n≥8/group, mean±SD). (C) Relative quantification of TCRβ or TCRγδ expression on either CD3$^-$NK1.1$^+$, CD3$^-$NK1.1$^-$ or CD3$^+$NK1.1$^+$ splenocytes from diseased N642H$^{NK/NK}$ mice (n=7). (D) Flow cytometric analysis of GFP$^+$ cells in the spleen of Cre neg, GFP$^{NK/NK}$, STAT5B$^{NK/NK}$, non-diseased N642H$^{NK/NK}$ and diseased N642H$^{NK/NK}$ mice (n≥8/group, mean±SD). Heatmap depicts percentage of GFP$^+$ cells out of living cells, percentages of DN (double-negative, CD27$^-$CD11b$^-$), CD27$^+$, DP (double-positive, CD27$^+$CD11b$^+$), CD11b$^+$, CD49a$^+$, CD49b$^+$ and KLRG1$^+$ cells out of GFP$^+$ NK cells (CD3$^-$NK1.1$^+$) and median fluorescence intensity (MFI) of NKp46, KLRG1 and NKG2D on GFP$^+$ NK cells. (E-F) Absolute values of flow cytometric analysis of GFP$^+$ NK cells in the (E) spleen, corresponding to heatmap data in Figure S5D, and in (F) liver, corresponding to heatmap data in Figure 5F, of aged non-diseased N642H$^{NK/NK}$ and diseased N642H$^{NK/NK}$ mice (n≥8/group, mean±SD). (*Left*) Percentages of DN (double-negative, CD27$^-$CD11b$^-$), CD27$^+$, DP (double-positive, CD27$^+$CD11b$^+$), CD11b$^+$, CD49a$^+$, CD49b$^+$ and KLRG1$^+$ cells out of GFP$^+$ NK cells (CD3$^-$NK1.1$^+$) and (*Right*) MFI of NKp46, KLRG1 and NKG2D on GFP$^+$ NK cells.

Levels of significance were calculated using one-way ANOVA in (A) and (B) and using unpaired t-test in (E) and (F). *p < 0.05, **p < 0.01, ***p < 0.001, ****p < 0.0001.

Figure S6: *STAT5B*^{N642H} induces transplantable NK-cell leukemia in mice

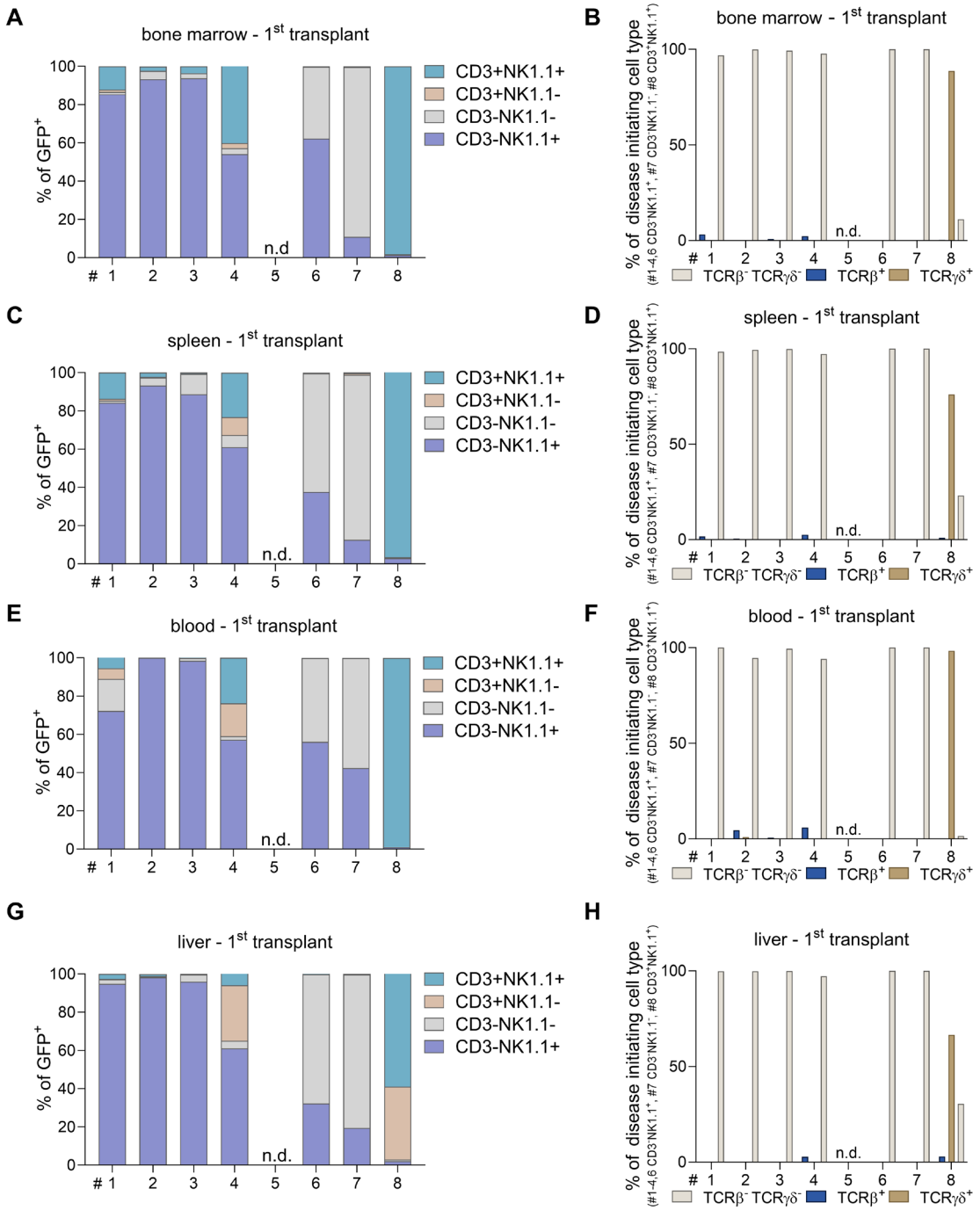

Figure S6: *STAT5B*^{N642H} induces transplantable NK-cell leukemia in mice

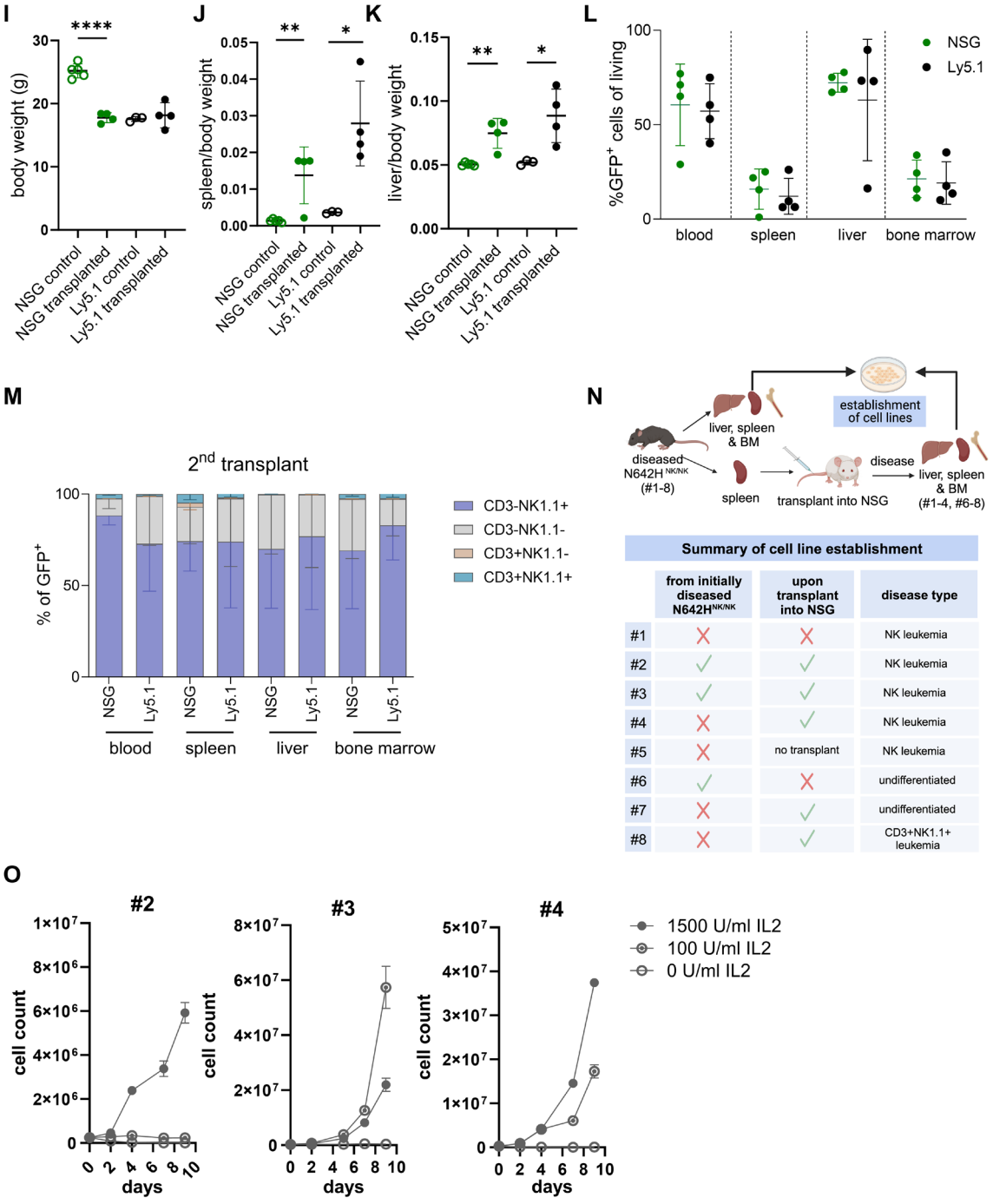

Summary of cell line establishment

	from initially diseased N642H$^{NK/NK}$	upon transplant into NSG	disease type
#1	✗	✗	NK leukemia
#2	✓	✓	NK leukemia
#3	✓	✓	NK leukemia
#4	✗	✓	NK leukemia
#5	✗	no transplant	NK leukemia
#6	✓	✗	undifferentiated
#7	✗	✓	undifferentiated
#8	✗	✓	CD3+NK1.1+ leukemia

Figure S6. *STAT5B*^{N642H} induces transplantable NK-cell leukemia in mice

Relative quantification of $CD3^+NK1.1^-$ T cells, $CD3^+NK1.1^+$ NKT cells, $CD3^-NK1.1^+$ NK and $CD3^-NK1.1^-$ cells among GFP^+ cells in (A) BM, (C) spleen, (E) blood and (G) liver of diseased NSG recipients transplanted (1st transplant) with diseased $N642H^{NK/NK}$ splenocytes (n=7). Relative quantification of TCRβ or TCRγδ expression on either $CD3^-NK1.1^+$, $CD3^-NK1.1^-$ or $CD3^+NK1.1^+$ cells in (B) BM, (D) spleen, (F) blood and (H) liver of diseased NSG recipients transplanted with diseased $N642H^{NK/NK}$ splenocytes (n=7). Quantification of (I) body weight, (J) spleen to body weight ratio and (K) liver to body weight ratio of diseased $N642H^{NK/NK}$ transplanted NSG and Ly5.1 mice and untransplanted controls (n≥3/group, mean±SD) (2nd transplant). (L) Flow cytometric analysis of percentage of GFP^+ cells in different tissues of NSG and Ly5.1 mice transplanted with splenocytes from the first round of diseased $N642H^{NK/NK}$ transplanted NSG mice (n=4/genotype, mean±SD). (M) Relative quantification of $CD3^+NK1.1^-$ T cells, $CD3^+NK1.1^+$ NKT cells, $CD3^-NK1.1^+$ NK cells and $CD3^-NK1.1^-$ "undifferentiated" cells among GFP^+ cells in different organs of diseased NSG and Ly5.1 recipients (n=4/genotype, mean±SD). (N) Schematic overview of establishment of stable cell lines from different organs of diseased $N642H^{NK/NK}$ mice or of diseased $N642H^{NK/NK}$ transplanted NSG mice. (O) Analysis of cytokine-dependent growth of three different $N642H^{NK/NK}$ cell lines (#2 and #3 established from splenocytes of initially diseased $N642H^{NK/NK}$ mice; #4 established from liver of diseased $N642H^{NK/NK}$ transplanted NSG mouse) upon culture with 1500 U/ml, 100 U/ml or 0 U/ml IL-2.

Levels of significance were calculated using unpaired t-test in (I)-(K). *$p < 0.05$, **$p < 0.01$, ****$p < 0.0001$.

Figure S7: Diseased N642H$^{NK/NK}$ NK cells display molecular features of NK-cell leukemia patients harboring *STAT5B* GOF mutations

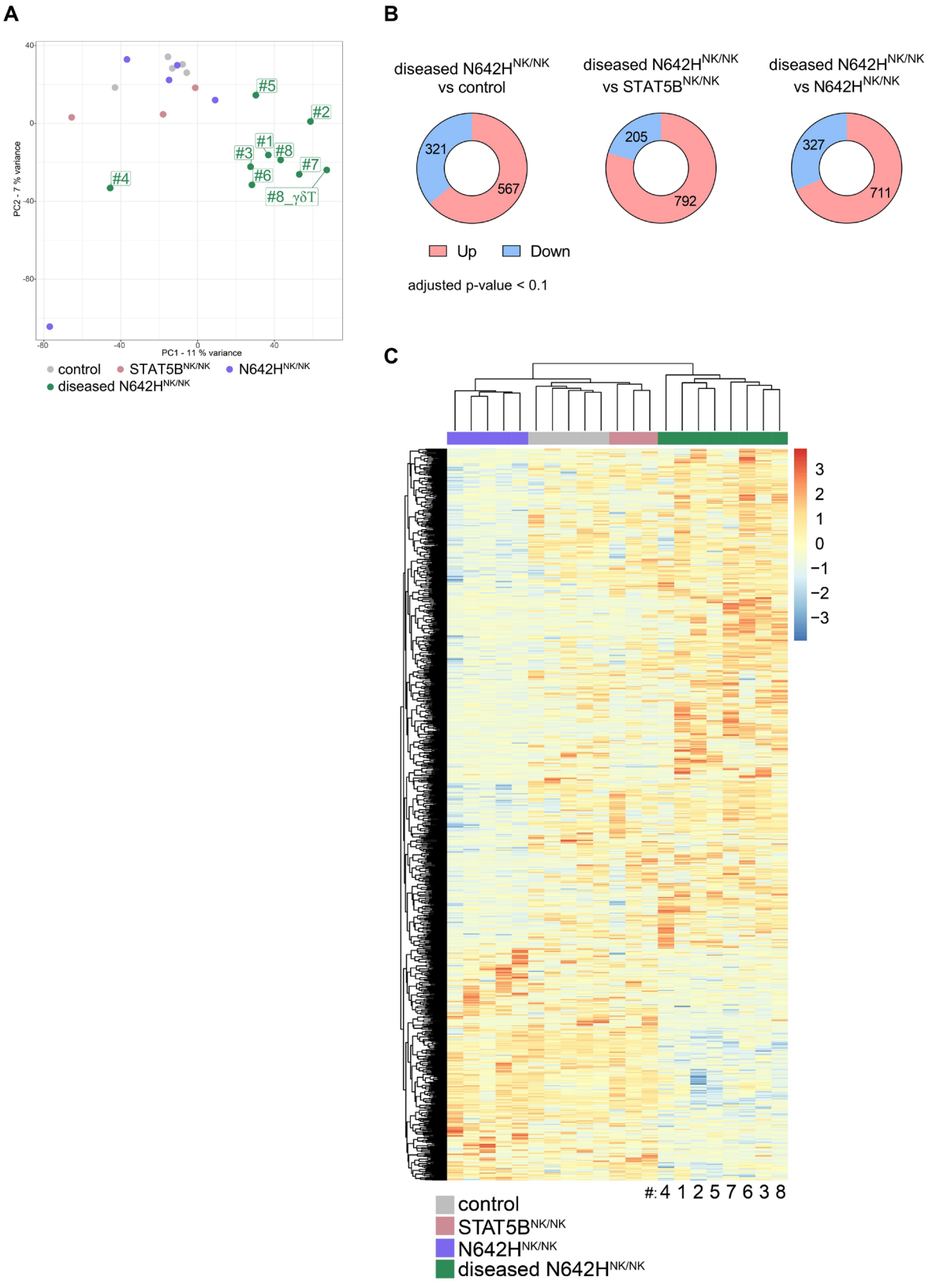

Figure S7: Diseased N642H$^{NK/NK}$ NK cells display molecular features of NK-cell leukemia patients harboring *STAT5B* GOF mutations

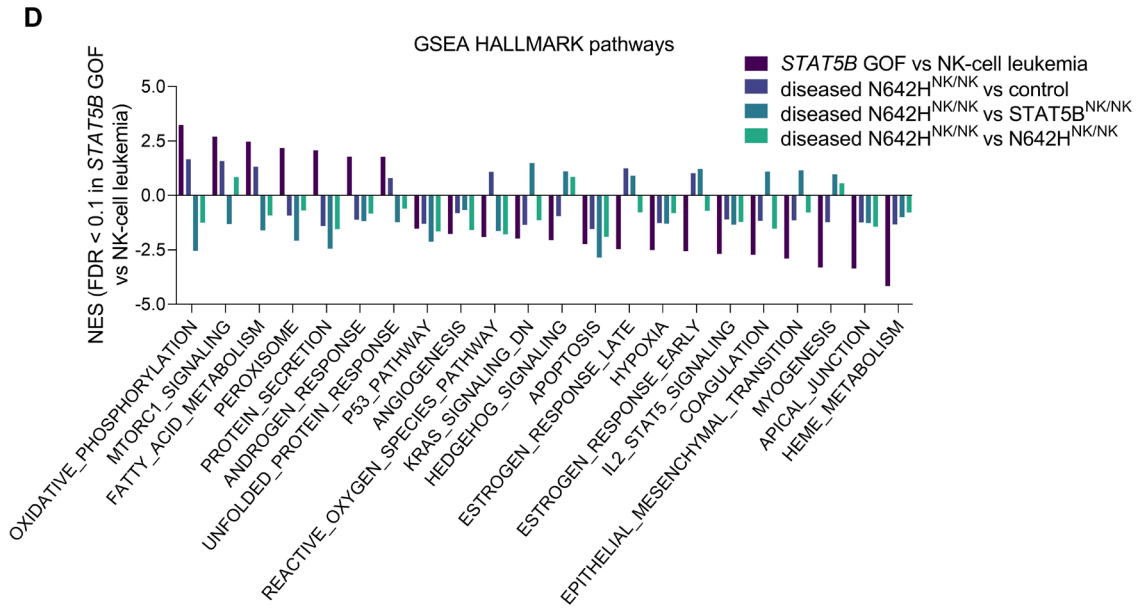

Figure S7. Diseased N642H$^{NK/NK}$ NK cells display molecular features of NK-cell leukemia patients harboring *STAT5B* GOF mutations

(A) PCA of RNA-sequencing data of aged control (Cre neg and GFP$^{NK/NK}$ (n=5)), STAT5B$^{NK/NK}$ (n=3), N642H$^{NK/NK}$ (n=5) and diseased N642H$^{NK/NK}$ (n=8) NK cells and γδT cells of #8 (n=1). (B) Donut plots illustrating numbers of significant (adjusted p-value <0.1) up- and downregulated DEGs from diseased N642H$^{NK/NK}$ (n=8) vs control (n=5), or vs. STAT5B$^{NK/NK}$ (n=3), or vs N642H$^{NK/NK}$ (n=5) NK cells. (C) Heatmap illustrating expression of the common DEGs from the comparison: diseased N642H$^{NK/NK}$ (n=8) vs. N642H$^{NK/NK}$ (n=5), in NK cells from control (n=5), STAT5B$^{NK/NK}$ (n=3), N642H$^{NK/NK}$ (n=5) and diseased N642H$^{NK/NK}$ (n=8) mice. (D) GSEA of HALLMARK pathways comparing diseased N642H$^{NK/NK}$ (n=8) vs control (n=5), or vs. STAT5B$^{NK/NK}$ (n=3), or vs N642H$^{NK/NK}$ (n=5) NK cells, and NK-cell leukemia (*STAT5B* GOF) (n=3) vs. NK-cell leukemia (n=44) patient samples. Quantification of the NES from 22 HALLMARK pathways with an FDR<0.1 in NK-cell leukemia (*STAT5B* GOF) (n=3) vs. NK-cell leukemia (n=44), but not in diseased N642H$^{NK/NK}$ (n=8) vs control (n=5) as indicated in **Figure 7D**.

Supplementary References

1. Ogilvy S, Metcalf D, Print CG, et al. Constitutive Bcl-2 expression throughout the hematopoietic compartment affects multiple lineages and enhances progenitor cell survival. *Proc. Natl. Acad. Sci. U. S. A.* 1999;96(26):14943–8.

2. Eckelhart E, Warsch W, Zebedin E, et al. A novel Ncr1-Cre mouse reveals the essential role of STAT5 for NK-cell survival and development. *Blood*. 2011;117(5):1565–73.

3. Mähler M, Berar M, Feinstein R, et al. FELASA recommendations for the health monitoring of mouse, rat, hamster, guinea pig and rabbit colonies in breeding and experimental units. *Lab. Anim.* 2014;48(3):178–192.

4. Yagita M, Huang CL, Umehara H, et al. A novel natural killer cell line (KHYG-1) from a patient with aggressive natural killer cell leukemia carrying a p53 point mutation. *Leuk. 2000 145*. 2000;14(5):922–930.

5. Chen IM, Whalen M, Bankhurst A, et al. A new human natural killer leukemia cell line, IMC-1. A complex chromosomal rearrangement defined by spectral karyotyping: Functional and cytogenetic characterization. *Leuk. Res.* 2004;28(3):275–284.

6. Bolger AM, Lohse M, Usadel B. Trimmomatic: A flexible trimmer for Illumina sequence data. *Bioinformatics*. 2014;30(15):2114–2120.

7. Smith T, Heger A, Sudbery I. UMI-tools: modeling sequencing errors in Unique Molecular Identifiers to improve quantification accuracy. *Genome Res.* 2017;27(3):491–499.

8. Dobin A, Davis CA, Schlesinger F, et al. STAR: Ultrafast universal RNA-seq aligner. *Bioinformatics*. 2013;29(1):15–21.

9. Frankish A, Diekhans M, Ferreira AM, et al. GENCODE reference annotation for the human and mouse genomes. *Nucleic Acids Res.* 2019;47(D1):D766–D773.

10. Liao Y, Smyth GK, Shi W. The Subread aligner: fast, accurate and scalable read mapping by seed-and-vote. *Nucleic Acids Res.* 2013;41(10):e108–e108.

11. R: a language and environment for statistical computing.

12. Love MI, Huber W, Anders S. Moderated estimation of fold change and dispersion for RNA-seq data with DESeq2. *Genome Biol.* 2014;15(12):550.

13. Subramanian A, Tamayo P, Mootha VK, et al. Gene set enrichment analysis: A knowledge-based approach for interpreting genome-wide expression profiles. *Proc. Natl. Acad. Sci. U. S. A.* 2005;102(43):15545–15550.

14. Mootha VK, Lindgren CM, Eriksson KF, et al. PGC-1α-responsive genes involved in oxidative phosphorylation are coordinately downregulated in human diabetes. *Nat. Genet. 2003 343*. 2003;34(3):267–273.

15. Liberzon A, Birger C, Thorvaldsdóttir H, et al. The Molecular Signatures Database (MSigDB) hallmark gene set collection. *Cell Syst.* 2015;1(6):417–425.

16. Liberzon A, Subramanian A, Pinchback R, et al. Molecular signatures database (MSigDB) 3.0. *Bioinformatics*. 2011;27(12):1739–1740.

Annex

Part I: Uncropped WB membranes

Figure 1A

3 8%-polyacrylamide gels have been loaded with the same lysates. The membranes has been cut at the 70 kDa protein ladder signal. The respective loading control for each blot is shown on the right.